International Journal of Thermophysics, Vol. 19, No. 2, 1998

Measurements of the Thermal Diffusivity Tensor of Polymer–Carbon Fiber Composites by Photothermal Methods[1]

A. Salazar[2, 3] and A. Sánchez-Lavega[2]

The thermal diffusivity tensor of a polymer–carbon fiber composite with unidirectionally distributed fibers has been measured using a modulated photothermal mirage device. The thermal diffusivity along the fibers is $k_{||} = 6.0 \pm 0.5\ \text{mm}^2 \cdot \text{s}^{-1}$, that perpendicular to the fibers is $k_{\perp} = 0.35 \pm 0.05\ \text{mm}^2 \cdot \text{s}^{-1}$, and that perpendicular to the sample surface is $k_z = 0.40 \pm 0.15\ \text{mm}^2 \cdot \text{s}^{-1}$. These results have been confirmed by independent measurements on the sample by other laboratories using three other different photothermal techniques. A previous claim on anomalous results found on this sample ($k_{||} < k_{\perp}$ and high thermal diffusivities) can be explained by the inappropriate use of the frequency range. We have also found that there is not perfect thermal contact between the fibers and the matrix, which can be characterized by the thermal contact resistance of $R_{\text{th}} = (9 \pm 2) \times 10^{-6}\ \text{m}^2 \cdot \text{K} \cdot \text{W}^{-1}$.

KEY WORDS: anisotropy; modulated photothermal techniques; polymer–carbon composites; thermal diffusivity tensor.

1. INTRODUCTION

Modulated photothermal techniques are based on the detection of the physical effects produced in a material because of the absorption of photons. During the last two decades numerous laboratories have used these techniques as efficient tools to measure the thermal parameters of solids, liquids, and gases [1, 2]. In particular, the thermal diffusivity of homogeneous and isotropic materials can be easily obtained through

[1] Paper presented at the Thirteenth Symposium on Thermophysical Properties, June 22–27, 1997, Boulder, Colorado, U.S.A.

[2] Departamento de Física Aplicada I, E.T.S. de Ingenieros Industriales y de Telecomunicación, Universidad del País Vasco, Alameda Urquijo s/n, 48013 Bilbao, Spain.

[3] To whom correspondence should be addressed.

0195-928X/98/0300-0625$15.00/0 © 1998 Plenum Publishing Corporation

several linear relations between experimental parameters (photothermal signal versus modulation frequency or versus distance between exciting and measurement points) [3]. The same methods are valid for the thermal diffusivity of homogeneous but anisotropic materials along their principal axes, although care must be taken when measuring the thermal diffusivity along any other direction [4, 5]. Moreover, an inverse procedure must be used to obtain the thermal diffusivity tensor when the principal axes are buried beneath the sample surfaces [6]. In recent years, several photothermal laboratories have focused their efforts on finding reliable photothermal methods to retrieve the thermal parameters of inhomogeneous materials, for example, thin films, multilayered systems, and composite materials (see Refs. 7 and 8 for an overview).

In this paper, we deal with a polymer–carbon fiber composite, which is an inhomogeneous and anisotropic material due to the unidirectional distribution of the fibers that reinforce the polymer. Our attention was attracted by the unexpected results of measurements of the thermal diffusivity tensor of this material that were published recently [9]. These authors found a higher value for the thermal diffusivity in the direction perpendicular to the fibers ($k_{\perp} = 71\ \text{mm}^2 \cdot \text{s}^{-1}$) than in the direction parallel to them ($k_{||} = 25\ \text{mm}^2 \cdot \text{s}^{-1}$). In addition, both quantities are too high for a composite based on a polymeric matrix ($k = 0.6\ \text{mm}^2 \cdot \text{s}^{-1}$). To clarify these previous anomalous results, measurements of the thermal diffusivity of this material along the three principal axes have been performed using the mirage technique as these authors did. Our results have been contrasted and complemented with measurements on the same sample, kindly supplied by outside laboratories, using three photothermal techniques: photoacoustic, photopyroelectric, and infrared radiometry. A comparison of this set of measurements allows us to establish the experimental conditions (modulation frequency and probe beam height) and sample characteristics (thickness, fiber diameter, etc.) to retrieve a reliable value of the "effective" thermal diffusivity of this kind of material.

Finally, we have made a first attempt to correlate the measured thermal diffusivity of the composite with the thermal parameters of both the matrix and the fiber. The results we have obtained indicate the presence of an imperfect thermal contact between the fibers and the matrix. An estimate of the average thermal resistance based on a simple model is presented.

2. SAMPLE DESCRIPTION

The polymer–carbon fiber composite studied is a preimpregnated ply (prepreg) based on poly(ether–ether–ketone) from ICI (PEEK) as polymeric

matrix. The carbon fibers are AS4 continuous fibers from Hercules. The prepreg composite system of PEEK/AS4 was used as supplied by the manufacturer with a composition of about 62 vol% carbon fibers. In Fig. 1 we show a scanning electron microscopy (SEM) micrograph of the cross section of the sample. As can be seen, the upper surface is rougher than the lower one. Thus the thickness of the sample is defined with a noticeable lack of precision to be $l = 0.175 \pm 0.015$ mm. Because some of the photothermal methods used to retrieve the thermal diffusivity in the direction perpendicular to the sample surface (k_z) make use of the value of the square of the sample thickness, the measured value of k_z will be affected by a severe error which is independent of the accuracy of the photothermal signal.

On the other hand, the SEM micrograph shows that fibers are distributed quite homogeneously, with an average diameter of 8 μm. This parameter will limit the experimental conditions under which an "effective" thermal diffusivity tensor ($k_{||}$, $k_{\perp}$, k_z) can be measured. The coordinate axes are defined in Fig. 2. In a modulated photothermal experiment, where highly damped thermal waves are generated, the magnitude that controls the distance traveled by the wave until its amplitude is decreased by a factor of e is the thermal diffusion length $\mu = (k/\pi f)^{1/2}$, where f is the modulation

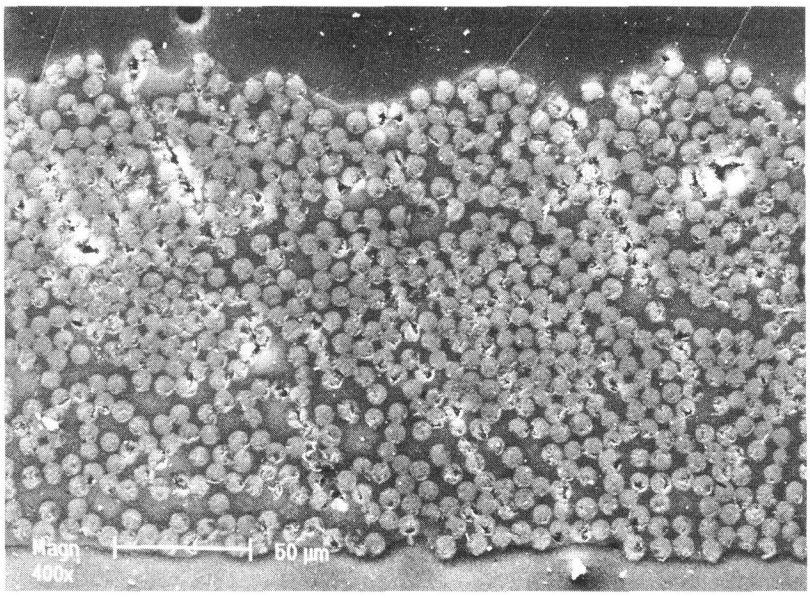

Fig. 1. SEM photograph of the cross section of the PEEK/AS4 sample.

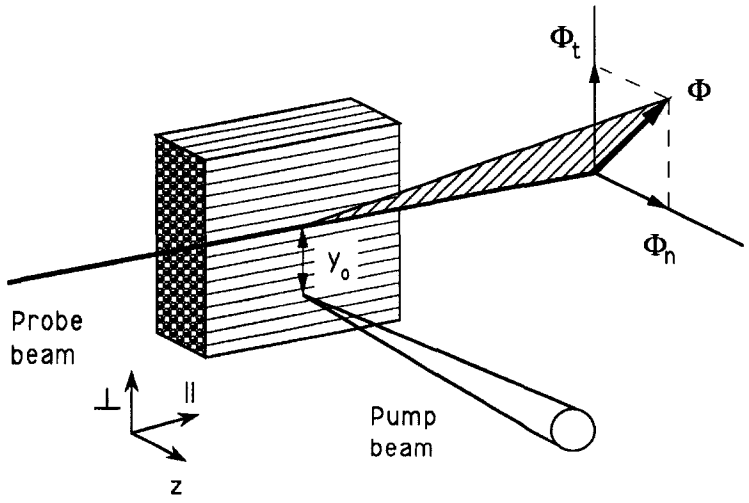

Fig. 2. Schematic of the mirage deflection geometry.

frequency. We can assert that at distances greater than 2μ or 3μ from the heating point, the thermal wave vanishes. In order to define an effective thermal diffusivity tensor for our anisotropic composite, the thermal diffusion length along each principal direction must be high enough to assure that several fibers are traversed by the thermal wave. This requires that $\mu \geqslant 20\,\mu$m in our case. Accordingly, the modulation frequency must be selected to accomplish this condition, taking into account that the thermal diffusivity of the material is very low.

3. RESULTS

In Fig. 2 we show the geometry of a perpendicular mirage setup. A modulated laser beam periodically heats the sample surface. A second laser beam is sent parallel to the sample surface at height z_o and transverse offset y_o with respect to the pump beam. This probe laser is deflected periodically due to the gradient of the refractive index in the surrounding gas. The mirage deflection has two components: the transverse deflection (ϕ_t), parallel to the sample surface; and the normal deflection (ϕ_n), perpendicular to the sample surface. A silicon quadrant detector connected to a lock-in amplifier is used to measure both components of the periodic mirage deflection. Two types of studies have been performed with the mirage device.

3.1. Nondestructive Evaluation: Composite Structure

Photothermal techniques can supplement the data provided by optical imaging because the scattering of the thermal waves carries information on the sample surface and subsurface buried structures. When the normal component of the mirage deflection (ϕ_n) is recorded while scanning the sample surface, with both heating and probe beams superimposed, two studies can be performed: at high frequencies ($f > 1$ kHz) a topography of the surface is obtained, but at low frequencies ($f < 100$ Hz) subsurface features (delaminations, inclusions, voids, etc.) can be detected. The behavior of the amplitude and phase of ϕ_n when scanning the PEEK/AS4 sample in the direction perpendicular to the fibers is shown in Fig. 3. A range of frequencies from 20 to 1280 Hz was employed. At the highest frequency, a quasi-periodic structure with peak-to- peak separation of 60 μm can be seen in both amplitude and phase. Bertolotti et al. [9] have interpreted this behavior as due to the existence of fiber bundles in which the thermal resistivity among fibers would be low. In this case, the fiber bundles would have a thermal conductivity higher than the polymeric material surrounding them. The photothermal response of buried independent cylindrical structures with different thermal properties from the matrix has been studied both theoretically and experimentally [10–12]. In the case of cylinders with a higher thermal conductivity and diffusivity than the matrix, the photothermal signal is characterized by a decrease in the amplitude, along with an increase in the phase above the cylinder. However, in all the scans shown in Fig. 3 both amplitude and phase have the same trend. We conclude that there is no evidence, either from SEM micrographs or from the mirage topography, of the existence of fiber bundles that could explain the anomalous thermal diffusivities reported previously. Fibers are distributed in the matrix homogeneously, and the quasi-periodic structure revealed in the mirage scan must be associated to a quasi-periodic surface roughness, as evident from the high-frequency scan.

3.2. The Thermal Diffusivity Tensor

In a classical modulated mirage experiment with point-like excitation there exists a linear relation between the phase of ϕ_t and the transverse distance (y_o) between the pump and the probe beams. The slope (m) of this linear relation allows us to retrieve the thermal diffusivity of the material through the equation [3]

$$m = -\sqrt{\frac{\pi f}{k}} \tag{1}$$

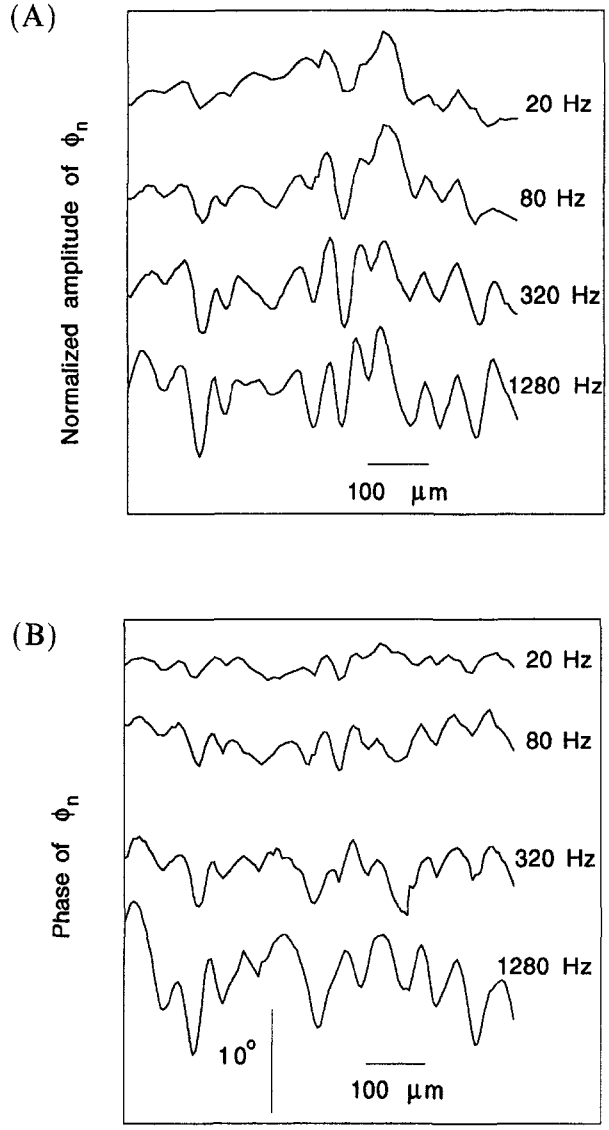

Fig. 3. Behavior of the amplitude (A) and phase (B) of the normal component of the mirage deflection when scanning the composite in the direction perpendicular to the fibers. Both the pump and the probe beams are superimposed.

However, this equation holds only for $z_o = 0$. For a more realistic configuration with $z_o \neq 0$, the direct application of Eq. (1) gives an erroneous value of k which is worse as k decreases. To overcome this limitation, the following improvements have been proposed [3, 13, 14]: (a) the use of very low frequencies, (b) the reflection of the probe beam on the sample surface (bouncing configuration), and (c) the introduction of corrections to the thermal diffusivity obtained directly from Eq. (1). In any case, both equations are also valid for anisotropic materials [5]. Figure 4 shows our

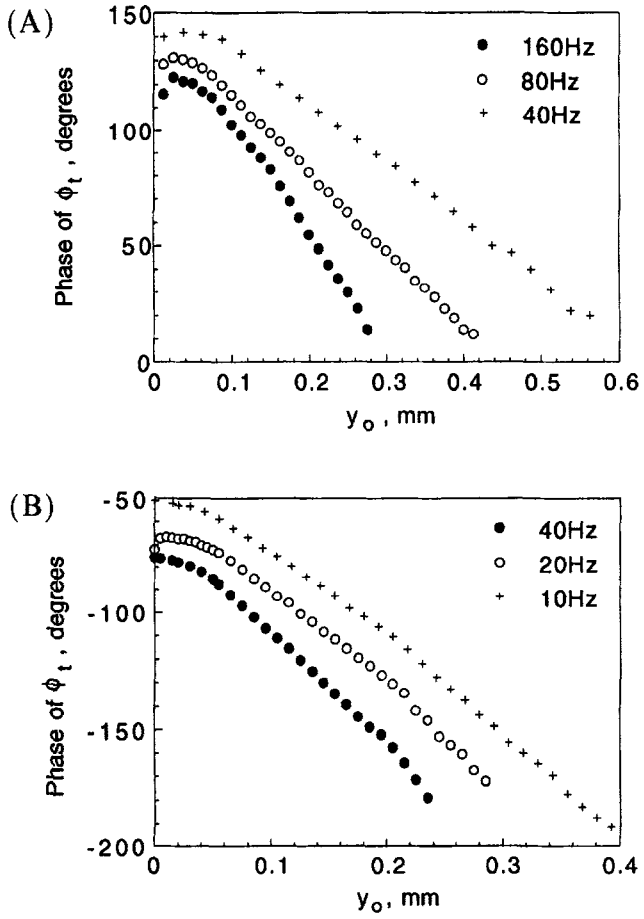

Fig. 4. Experimental measurements of the phase of the transverse component of the mirage deflection as a function of the transverse distance between the pump and the probe beams (y_o): (A) y_o is parallel to the fibers; (B) y_o is perpendicular to the fibers.

experimental measurements. Using this method we have found $k_{||} = 6.0 \pm 0.5\ \mathrm{mm^2 \cdot s^{-1}}$ and $k_{\perp} = 0.35 \pm 0.05\ \mathrm{mm^2 \cdot s^{-1}}$. For the former, we employed frequencies ranging from 40 to 160 Hz, while for the later, frequencies lower than 40 Hz were necessary.

A different methodology must be used to measure the thermal diffusivity perpendicular to the sample surface (k_z) with a mirage device. In this case, the probe beam scans both the illuminated (front) and the nonilluminated (back) surfaces. When the material is thermally thick, i.e., for frequencies higher than the critical frequency $f_c = k_z/l^2$, a linear relation is found when plotting the phase difference of ϕ_n in the rear and in the front surfaces, as a function of $f^{1/2}$. A similar linear relation holds when plotting the logarithm of the ratio of the magnitudes of ϕ_n in the back and front surfaces as a function of $f^{1/2}$. The slope of both linear relations (m') is related to the thermal diffusivity perpendicular to the sample surface through the equation [15]

$$m' = l\sqrt{\frac{\pi}{k_z}} \tag{2}$$

This relation is independent of z_o. Although most authors have used planar excitation, we have obtained better results with pump beam radii in the range from 0.1 to 0.5 mm. The measurements are shown in Fig. 5. The value of k_z we have obtained by this method is $k_z = 0.40 \pm 0.15\ \mathrm{mm^2 \cdot s^{-1}}$. This value is affected by an error that depends not only on the accuracy of

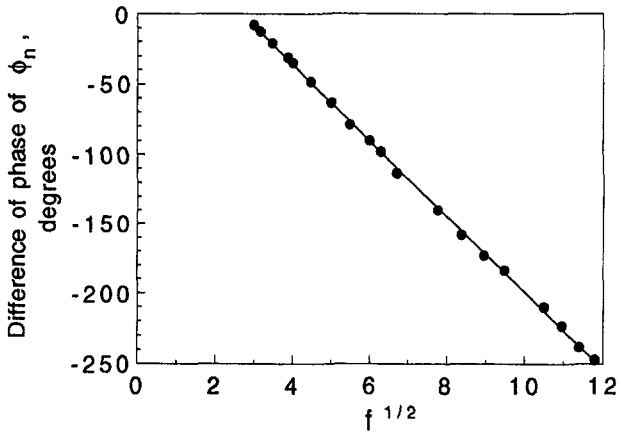

Fig. 5. Experimental measurements of the phase difference between the phase of the normal component at the illuminated and that at the nonilluminated surfaces as a function of $f^{1/2}$.

the mirage measurements but also on the uncertainty in the value of the sample thickness.

In order to validate our results, measurements of the elements of the diffusivity tensor have been performed on the same sample in outside laboratories using three photothermal techniques: (a) infrared radiometry ($k_{||} = 4 \pm 1\ \text{mm}^2 \cdot \text{s}^{-1}$; $k_{\perp} = 0.4 \pm 0.1\ \text{mm}^2 \cdot \text{s}^{-1}$), (b) photoacoustic ($k_z = 0.27\ \text{mm}^2 \cdot \text{s}^{-1}$), and (c) photopyroelectric ($k_z = 0.5 \pm 0.2\ \text{mm}^2 \cdot \text{s}^{-1}$). However, we have to recognize that only the mirage technique is able to measure the three components of the thermal diffusivity tensor. From these results we can conclude that photothermal techniques are very useful tools to measure the thermal diffusivity tensor of heterogeneous and anisotropic samples. In any case, care must be taken with the modulation frequency selected. In order to average the inhomogeneity introduced by the fibers, reliable photothermal measurements of heterogeneous fiber composites require the thermal diffusion length (μ) to be larger than the distance between adjacent fibers. In our sample, the average distance between adjacent fibers is of the order of $10\,\mu$m, so thermal diffusion lengths lower than $20\,\mu$m must be avoided. Taking into account the low values of $k_{\perp}$ and k_z, this condition imposes an upper limit of about 250 Hz to the modulation frequency we can use. However, this is not a very restrictive condition, because reliable application of Eq. (1) requires the use of frequencies as low as possible. In our case, frequencies higher than 40 Hz in the measurement of $k_{\perp}$ and than 160 Hz in the measurement of $k_{||}$ were avoided because of the lack of linearity appearing in the above mirage relations. As a general conclusion from this discussion we can say that previous claims [9], indicating $k_{||} < k_{\perp}$ and absolute values for $k_{||}$ and $k_{\perp}$ one order higher than those we have found, must be disregarded.

4. ANALYSIS

In this section we try to correlate the thermal diffusivity values we have obtained for this composite with the thermal properties of both the matrix and the fibers. The thermal conductivity and diffusivity of the matrix (PEEK) are $K_m = 0.25\ \text{W} \cdot \text{m}^{-1} \cdot \text{K}^{-1}$ and $k_m = 0.60\ \text{mm}^2 \cdot \text{s}^{-1}$, respectively [16]. Unfortunately we do not know the thermal properties of the carbon fibers, but the ratio between their thermal conductivity and their thermal diffusivity must be of the order of $K_f/k_f = (1.35 \pm 0.05) \times 10^6\ \text{W} \cdot \text{s} \cdot \text{m}^{-3} \cdot \text{K}^{-1}$ [17].

Let us first introduce the following relations and definitions [18]: (a) the thermal wave impedance is a complex quantity defined as the ratio of the temperature to the heat flux density, $Z = (i2f\rho CK)^{-1/2}$, where ρ is the density and C is the specific heat; (b) the relation between the thermal

diffusivity and the thermal conductivity is $k = K/\rho C$; (c) the effective heat capacity of the composite follows the rule of any mixture: $\rho C = V_f \rho_f C_f + V_m \rho_m C_m = V_f(K_f/k_f) + V_m(K_m/k_m)$, where V_f and V_m are the volume fraction of fibers and matrix, respectively; (d) the thermal conductivity parallel to the unidirectionally oriented fibers is not affected by the presence of interfacial thermal barrier resistances between fibers and matrix and can be calculated as the effective thermal conductivity of two thermal resistors in parallel, $K_{||} = V_f K_f + V_m K_m$; and (e) a general expression for the thermal conductivity perpendicular to the fibers does not exist. Moreover, the thermal conductivity in this direction is strongly affected by the presence of interfacial thermal barriers. The lowest possible value of this quantity, in the absence of interfacial thermal barriers, is obtained assuming a thermal resistor in series model: $1/K_\perp(\text{lowest}) = (V_f/K_f) + (V_m/K_m)$.

Using the above results, we can obtain the expression for the thermal diffusivity parallel to the fibers ($k_{||}$) and a lower limit for the thermal diffusivity perpendicular to the fibers $k_\perp$(lowest):

$$k_{||} = \frac{V_f K_f + V_m K_m}{V_f(K_f/k_f) + V_m(K_m/k_m)} \tag{3}$$

$$k_\perp(\text{lowest}) = \frac{K_f K_m}{(V_f K_m + V_m K_m)[V_f(K_f/k_f) + V_m(K_m/k_m)]} \tag{4}$$

Using Eq. (3) with our experimental value of $k_{||} = 6.0 \pm 0.5\ \text{mm}^2 \cdot \text{s}^{-1}$ and K_f/k_f as above, we get for the fibers $K_f = 9.5 \pm 1.1\ \text{W} \cdot \text{m}^{-1} \cdot \text{K}^{-1}$ and $k_f = 7.0 \pm 0.6\ \text{mm}^2 \cdot \text{s}^{-1}$. Introducing these values in Eq. (4) we get a lower limit for the thermal diffusivity perpendicular to the fibers: $k_\perp(\text{lowest}) = 0.63 \pm 0.02\ \text{mm}^2 \cdot \text{s}^{-1}$, which is higher than the experimental value we have retrieved. The latter result can be explained by the existence of an imperfect thermal contact between the fibers and the matrix, which can be characterized by a contact thermal resistance (R_{th}). In order to estimate its value, we used the expression for the thermal conductivity perpendicular to the fibers proposed by Hasselman and Johnson [see Eq. (11) in Ref. 19], which allows us to calculate the thermal diffusivity perpendicular to the fibers:

$$k_\perp = \frac{K_m}{V_f(K_f/k_f) + V_m(K_m/k_m)} \frac{K_f(1+\alpha) + K_m + V_f[K_f(1-\alpha) - K_m]}{K_f(1+\alpha) + K_m - V_f[K_f(1-\alpha) - K_m]} \tag{5}$$

where $\alpha = K_m/R_{\text{th}}/a$ and a is the fiber radius.

Using our experimental value of $k_{\perp} = 0.35 \pm 0.05\ \mathrm{mm^2 \cdot s^{-1}}$ we obtain $\alpha = 0.55 \pm 0.15$, and taking into account that $a = 4\ \mu\mathrm{m}$ we get $R_{\mathrm{th}} = (9 \pm 2) \times 10^{-6}\ \mathrm{m^2 \cdot K \cdot W^{-1}}$. It should be noted that in Eq. (5) the volume fraction of the fiber is assumed to be sufficiently low that interactions between the local temperature fields of neighboring dispersions are absent. Because the volume fraction of the fibers in our composite is quite high, the above value for the contact thermal resistance must be regarded as tentative.

ACKNOWLEDGMENTS

We would like to acknowledge Dr. T. A. Ezquerra for kindly supplying us the sample measured in this paper. We are indebted to Dr. M. Marinelli from the Universitá di Roma Tor Vergata, Dr. J. J. Alvarado-Gil from CINVESTAV-IPN in Mexico, and Mr. J. F. Bisson from ESPCI in Paris for performing photothermal measurements. This work was supported by the Government of the Basque Country through Research Grant IP96/4.

REFERENCES

1. H. Vargas and L. C. M. Miranda, *Phys. Rep.* **161**:45 (1988).
2. H. K. Park, C. P. Grigoropoulos, and A. C. Tam, *Int. J. Thermophys.* **16**:973 (1995).
3. A. Salazar and A. Sánchez-Lavega, *Rev. Sci. Instrum.* **65**:2896 (1994).
4. A. Salazar, A. Sánchez-Lavega, A. Ocáriz, J. Guitonny, G. C. Pandey, D. Fournier, and A. C. Boccara, *Appl. Phys. Lett.* **67**:626 (1995).
5. A. Salazar, A. Sánchez-Lavega, A. Ocáriz, J. Guitonny, G. C. Pandey, D. Fournier, and A. C. Boccara, *J. Appl. Phys.* **79**:3984 (1996).
6. A. Salazar, A. Sánchez-Lavega, and A. Ocáriz, *Opt. Eng.* **36**:391 (1997).
7. Proceedings of the 9th international conference on photoacoustic and photothermal phenomena, in *Progress in Natural Science, Vol. 6 Suppl.*, S. Y. Zhang, ed. (Science in China Press, Beijing, 1996).
8. Proceedings of the 8th international conference on photoacoustic and photothermal phenomena, in *Journal de Physique IV, Colloque C7*, D. Fournier and J.P. Roger, eds. (1994).
9. M. Bertolotti, A. Ferrari, G. L. Liakhou, R. Li Voti, A. Marras, T. A. Ezquerra, and F. J. Balta-Calleja, *J. Appl. Phys.* **78**:5706 (1995).
10. L. D. Favro, P. K. Kuo, and R. L. Thomas, in *Photoacoustic and Photothermal Wave Phenomena in Semiconductors*, A. Mandelis, ed. (Elsevier, New York, 1987), p. 69.
11. A. Ocáriz, A. Sánchez-Lavega, and A. Salazar, *J. Appl. Phys.* **81**:7552 (1997).
12. A. Ocáriz, A. Sánchez-Lavega, and A. Salazar, *J. Appl. Phys.* **81**:7561 (1997).
13. M. Bertolotti, R. Li Voti, G. Liakhou, and C. Sibilia, *Rev. Sci. Instrum.* **64**:1576 (1993).
14. A. Salazar and A. Sánchez-Lavega, *Rev. Sci. Instrum.* **66**:275 (1995).

15. A. Skumanich, H. Dersch, M. Fathallah, and N. M. Amer, *Appl. Phys. A* **43**:297 (1987).
16. Goodfellow Cambridge Limited catalog (1995–1996), p. 478.
17. T. Yamane, S. Katayama, M. Todoki, and I. Hatta, *J. Appl. Phys.* **80**:4358 (1996).
18. J. E. Parrott and A. D. Stukes, *Thermal Conductivity in Solids* (Pion Limited, London, 1975), p. 129.
19. D. P. H. Hasselman and L. F. Johnson, *J. Comp. Mat.* **21**:508 (1987).

Printed in Belgium